# Multi-class Binary Symbol Classification with Circular Blurred Shape Models

Sergio Escalera[1,2], Alicia Fornés[1,3], Oriol Pujol[1,2], and Petia Radeva[1,2]

[1]Computer Vision Center, Campus UAB, edifici O, 08193, Bellaterra, Spain
[2]Dept. Matemàtica Aplicada i Anàlisi, UB, Gran Via 585, 08007, Barcelona, Spain
[3]Dept. Computer Science, Campus UAB, Edifici Q, 08193, Bellaterra, Spain

**Abstract.** Multi-class binary symbol classification requires the use of rich descriptors and robust classifiers. *Shape* representation is a difficult task because of several symbol distortions, such as occlusions, elastic deformations, gaps or noise. In this paper, we present the Circular Blurred Shape Model descriptor. This descriptor encodes the arrangement information of object parts in a correlogram structure. A prior blurring degree defines the level of distortion allowed to the symbol. Moreover, we learn the new feature space using a set of Adaboost classifiers, which are combined in the Error-Correcting Output Codes framework to deal with the multi-class categorization problem. The presented work has been validated over different multi-class data sets, and compared to the state-of-the-art descriptors, showing significant performance improvements.

## 1 Introduction

Shape Recognition is one of the most active areas in Pattern Recognition, which consists in recognizing objects from a large set of classes (we use symbol and object indistinctly). Shape is one of the most important visual cues for describing objects, and with texture and color, it is widely used for describing the content of the objects. In the last years, there is an increasing interest in the developing of good shape recognition methods. Shape representation is a difficult task because of several object distortions, such as occlusions, elastic deformations, gaps or noise. In general, the desirable properties of a shape-based approach can be divided in two main groups: the definition of expressive and compact shape descriptors, and the formulation of robust classification methods.

A good shape descriptor should guarantee inter-class compactness and intra-class separability, even when describing noisy and distorted shapes. The main techniques for shape recognition are reviewed in [2]. They are mainly classified in continuous and structural approaches. Zernike moments and R-signature are examples of continuous approaches, which extract information from the whole shape region. Zernike moments [3] maintain properties of the shape, and are invariant to rotation, scale, and deformations. Contrary, other continuous approaches only use the external contour (silhouette) for computing the features, such as Curvature Scale Space (CSS) and Shape context. CSS [5] is a standard of the MPEG [4] that is tolerant to rotation, but it can only be used for close curves. Shape Context can work with non-closed curves, and has good performance in hand drawn symbols, because it is tolerant to deformations, but it requires point-to-point alignment of the symbols [6].

Concerning structural approaches, straight lines and arcs are usually the basic primitives. Strings, graphs or trees represent the relations between these primitives. The similarity measure is performed by string, tree or graph matching. Attributed graph grammars, Deformable models and Region Adjacency Graphs are a few examples of structural approaches. Attributed graph grammars [7] can cope with partially occluded symbols, while Region Adjacency Graphs [8] reach good performance in front of distortions in hand drawn documents.

Due to the large different kinds of problems in shape recognition applications, a shape descriptor usually reaches good performance in some aspects, but fails in others. In fact, some object descriptors, robust to some affine transformations and occlusions in some type of objects, are not enough effective in front of elastic deformations. For this reason, the research of a descriptor that can cope with elastic deformations and non-uniform distortions is still required. In the work of [11], the blurred shape model was presented. It is a descriptor that can deal with elastic deformations, variations in object styles and blurring, but it is sensible to rotations. In this paper, we present an evolution of the blurred shape model descriptor, which not only copes with distortions and noise, but also is rotationally invariant. The Circular Blurred Shape Model (CBSM) codifies the spatial arrangement of object characteristics using a correlogram structure. Based on a prior blurring degree, object characteristics are shared among correlogram regions. By rotating the correlogram so that the major descriptor densities are aligned to the $x$-axis, the descriptor becomes rotationally invariant.

Referring the categorization of object classes, many classification techniques have been developed. One of the most well-known techniques is the Adaboost algorithm, which has been shown to be good for feature selection, and it has shown to achieve high performance when applied to binary categorization tasks [9]. Afterwards, the extension to the multi-class case is usually solved by combining the binary classifiers in a voting scheme, such as one-versus-one or one-versus-all grouping schemes. Dietterich et. al. [10] proposed the Error Correcting Output Codes framework (ECOC) to benefit from error correction properties, obtaining successful results [15]. In this paper, we learn the CBSM features using Adaboost, and then, combine the binary problems in an ECOC configuration, which extends the system to deal with multi-class categorization problems. The comparison with the state-of-the-art descriptors and the high performance classifying multi-class problems with several categories show the robustness and better performance of the present methodology.

The paper is organized as follows: Section 2 describes the rotationally invariant Circular Blurred Shape Model descriptor. Section 3 describes the system of Error-Correcting Output Codes that uses the CBSM system to solve multi-class categorization problems. Section 4 presents the experimental evaluation of the methodology, and finally, Section 5 concludes the paper.

## 2 Circular Blurred Shape Model

In order to describe an object that can suffer from irregular deformations, the authors of [11] proposed a description strategy in which spatial arrangement of object parts is captured in a rectangular grid. Contiguous regions share information about the containing object points, and thus, the descriptor is tolerant to irregular deformations. The descriptor has shown to be suitable for the multi-class categorization of aligned symbols, outperforming state-of-the-art strategies [11].

In this section, we present a circular formulation of the Blurred Shape Model descriptor (CBSM). By defining a correlogram structure from the center of the object region, spatial arrangement of object parts is shared among regions defined by circles and sections. The method also allows a rotationally invariant description, rotating the correlogram by the predominant region densities. We divide the description of the algorithm into three main steps: the definition of the correlogram parameters, the descriptor computation, and the rotationally invariant procedure. We also include a fourth step to extend the CBSM methodology to solve symbol spotting problems.

**Correlogram definition:** Given a number of circles $C$, number of sections $S$, and an image region $I$, a centered correlogram $B = \{b_{\{1,1\}}, .., b_{\{C,S\}}\}$ is defined as a radial distribution of sub-regions of the image, as shown in Figure 1(a) and (b). Each region $b$ has centroid coordinates defined by $b^*$. Then, the regions around $b$ are defined as the neighbors of $b$. Note that depending of the spatial location of the analyzed region, different number of neighbors can be defined (Fig. 1(c)).

**Descriptor computation:** In order to compute the descriptor, first, a preprocess of the input region $I$ to obtain the shape features is required. Working with document images, relevant *shape* information can be obtained by means of a contour map. However, based on the object properties, we can define another initial properties. In this paper, we use a Canny edge detector procedure.

Given the object contour map, each point from the image belonging to a contour is taken into account in the description process (Fig. 1(d)). First of all, the distances from the contour point $\mathbf{x}$ to the centroids of its corresponding region and neighbor regions are computed. The inverse of these distances are computed and normalized by the sum of total distances. These values are then added to the corresponding positions of the descriptor vector $\nu$, including higher values to that positions corresponding to the nearest regions to $\mathbf{x}$ (Figure 1(e) bottom). This makes the description tolerant to irregular deformations.

At this point we have a description $\nu$ for an input image $I$, where the length of $\nu$, defined by parameters $C$ and $S$, defines the degree of spatial information taken into account in the description process. In Figure 2, a bat instance from the public MPEG7 data set [1] is described with different $C \times S$ correlogram sizes. In the way that we increase the number of regions, the description becomes more local. Thus, an optimal parameters of $C$ and $S$ should be obtained for each particular problem (i.e. via cross-validation).

**Rotationally invariant descriptor:** In order to make the description rotationally invariant, we look for the main diagonal $G_i$ of correlogram $B$ with the highest density. This diagonal is then the reference to rotate the descriptor. The orientation of the rotationally process, so that $G_i$ is aligned with the $x$-axis, is that corresponding to the highest description density at both sides of $G_i$. This procedure is detailed in Algorithm 2. A visual result of the rotationally invariant process can be observed in Figure 2.

**Algorithm 1** Circular Blurred Shape Model Description Algorithm.

**Require:** a binary image $I$, the number of circles $C$, and the number of sections $S$
**Ensure:** descriptor vector $\nu$

**Define** $d = R/C$ and $g = 360/S$, where $R$ is the radius of the correlogram, as the distance between consecutive circles and the degrees between consecutive sectors, respectively (Figure 1(a)).
**Define** $B = \{b_{\{1,1\}}, .., b_{\{C,S\}}\}$ as the set of bins for the circular description of $I$, where $b_{c,s}$ is the bin of $B$ between distance $[(c-1)d, cd)$ with respect to the origin of coordinates $o$, and between angles $[(s-1)g, sg)$ to the origin of coordinates $o$ and $x$-axis (Figure 1(b)).
**Define** $b^*_{\{c,s\}} = (d \sin \alpha, d \cos \alpha)$, the centroid coordinates of bin $b_{\{c,s\}}$, where $\alpha$ is the angle between the centroid and the $x$-axis, and $B^* = \{b^*_{\{1,1\}}, .., b^*_{\{C,S\}}\}$ the set of centroids in $B$ (Figure 1(e)).
**Define** $X_{b_{\{c,s\}}} = \{b_1, .., b_{cs}\}$ as the sorted set of the elements in $B^*$ so that $d(b^*_{\{c,s\}}, b^*_i) \le d(b^*_{\{c,s\}}, b^*_j)$, $i < j$.
**Define** $N(b_{\{c,s\}})$ as the neighbor regions of $b_{\{c,s\}}$, defined by the initial elements of $X_{b_{\{c,s\}}}$:

$$N(b_{\{c,s\}}) = \begin{cases} X', |X'| = S+3 & \text{if } b_{\{c,s\}} \in IN \\ X', |X'| = 9 & \text{if } b_{\{c,s\}} \in MI \\ X', |X'| = 6 & \text{if } b_{\{c,s\}} \in EX \end{cases}$$

being $X'$ the first elements of $X$, and $IN$, $MI$, and $EX$, the inner, middle, and extern regions of $B$, respectively (Figure 1(c)). Note that different number of neighbor regions appears depending of the location of the region in the correlogram. We consider the own region as the first neighbor.
**Initialize** $\nu_i = 0$, $i \in [1, .., CS]$, where the order of indexes in $\nu$ are:
$\nu = \{b_{\{1,1\}}, .., b_{\{1,S\}}, b_{\{2,1\}}, ..b_{\{2,S\}}, .., b_{\{C,1\}}, ..b_{\{C,S\}}\}$
**for** each point $\mathbf{x} \in I$, $I(\mathbf{x}) = 1$ (Figure 1(d)) **do**
  **for** each $b_{\{i,j\}} \in N(b_{\mathbf{x}})$ **do**
    $d_{\{i,j\}} = d(\mathbf{x}, b_{\{i,j\}}) = ||\mathbf{x} - b^*_{\{i,j\}}||^2$
  **end for**
  Update the probabilities vector $\nu$ positions as follows (Figure 1(f)):
  $\nu(b_{\{i,j\}}) = \nu(b_{\{i,j\}}) + \frac{1/d_{\{i,j\}}}{D_{\{i,j\}}}$, $D_{\{i,j\}} = \sum_{b_{\{m,n\}} \in N(b_{\{i,j\}})} \frac{1}{||\mathbf{x} - b^*_{\{m,n\}}||^2}$
**end for**
Normalize the vector $\nu$ as follows:
$d' = \sum_{i=1}^{CS} \nu_i$, $\nu_i = \frac{\nu_i}{d'}, \forall i \in [1, .., CS]$

## 3 Multi-class Categorization

Error Correcting Output Codes are a meta-learning strategy that divides the multi-class problem is a set of binary problems, solves them individually and aggregates their responses into a final decision. ECOC classifiers combination have been shown to have interesting properties in statistical learning, reducing both the bias and variance of the base classifiers [12].

The ECOC meta-learning algorithm [13] consists in two steps: in the learning step, an ECOC encoding matrix is constructed in order to define the combination of the $M$ binary classifiers. In the decoding step, the new sample $\mathbf{x}$ is classified

**Algorithm 2** Rotationally invariant $\nu$ description.

**Require:** $\nu$, $S$, $C$
**Ensure:** Rotationally invariant descriptor vector $\nu^{ROT}$
**Define** $G = \{G_1, .., G_{S/2}\}$ the $S/2$ diagonals of $B$, where $G_i = \{\nu(b_{\{1,i\}}), .., \nu(b_{\{C,i\}}), .., \nu(b_{\{1,i+S/2\}}), .., \nu(b_{\{C,i+S/2\}})\}$

Select $G_i$ so that $\sum_{j=1}^{2C} G_i(j) \geq \sum_{j=1}^{2C} G_k(j)$, $\forall k \in [1, .., S/2]$

**Define** $L_G$ and $R_G$ as the left and right areas of the selected $G_i$ as follows:
$L_G = \sum_{j,k} \nu(b_{\{j,k\}}), j \in [1, .., C], k \in [i+1, .., i+S/2-1]$
$R_G = \sum_{j,k} \nu(b_{\{j,k\}}), j \in [1, .., C], k \in [i+S/2+1, .., i+S-1]$

**if** $L_G > R_G$ **then**
$B$ is rotated $k = i + S/2 - 1$ positions to the left:
$\nu^{ROT} = \{\nu(b_{\{1,k+1\}}), .., \nu(b_{\{1,S\}}), \nu(b_{\{1,1\}}), .., \nu(b_{\{1,k\}}), ..,$
$, .., \nu(b_{\{C,k+1\}}), .., \nu(b_{\{C,S\}}), \nu(b_{\{C,1\}}), .., \nu(b_{\{C,k\}})\}$
**else**
$B$ is rotated $k = i - 1$ positions to the right:
$\nu^{ROT} = \{\nu(b_{\{1,S\}}), .., \nu(b_{\{1,S-k+1\}}), \nu(b_{\{1,1\}}), .., \nu(b_{\{1,S-k\}}), ..,$
$, .., \nu(b_{\{C,S\}}), .., \nu(b_{\{C,S-k+1\}}), \nu(b_{\{C,1\}}), .., \nu(b_{\{C,S-k\}})\}$
**end if**

according to the set of $M$ binary classifiers. The decoding algorithm finds the most suitable class label for the test sample using the output of this binary set of classifiers. Thus, given a set of $N$ training samples $\mathbf{X} = \{\mathbf{x}_1, \ldots, \mathbf{x}_N\}$, where each $\mathbf{x}_i$ belongs to the class $C_i \in \{C_1, \ldots, C_K\}$, an ECOC encoding consists on constructing $M$ binary problems using the original $K$ classes. Each binary problem splits two meta-classes, and values +1 and -1 are assigned to each class belonging to the first or second meta-classes, respectively. If a class does not belong to any meta-class, the membership value is set to 0. This creates a $K \times M$ matrix $\mathbf{T}$. When a new sample must be classified, the outputs of the classifiers trained on each binary problem (columns of the matrix $\mathbf{T}$) are used to construct the codeword that is compared with each row of the matrix $\mathbf{T}$. The class codeword with the minimum distance is selected as the classifier output. The ECOC scheme allows to represent in a common framework well-known strategies such as one-versus-all or all-pairs, as well as more sophisticated problem dependent encodings, namely discriminant ECOC [14] or sub-class ECOC [15], without a significant increment of the codeword length. Literature shows that one of the most straightforward and well-performing approach disregarding of the properties of the particular base learner is the *one-versus-one* strategy.

The final part of the ECOC process is based on defining a suitable distance for comparing the output of the classifiers with the base codewords. The authors of [17] have recently shown that *weighted decoding* achieves the minimum error with respect to most of the state-of-the-art decoding measures. The weighted decoding strategy decomposes the decoding step of the ECOC technique in two parts: a weighting factor for each code position and any general decoding strategy. In [17] the authors show that for a decoding strategy to be successful, two

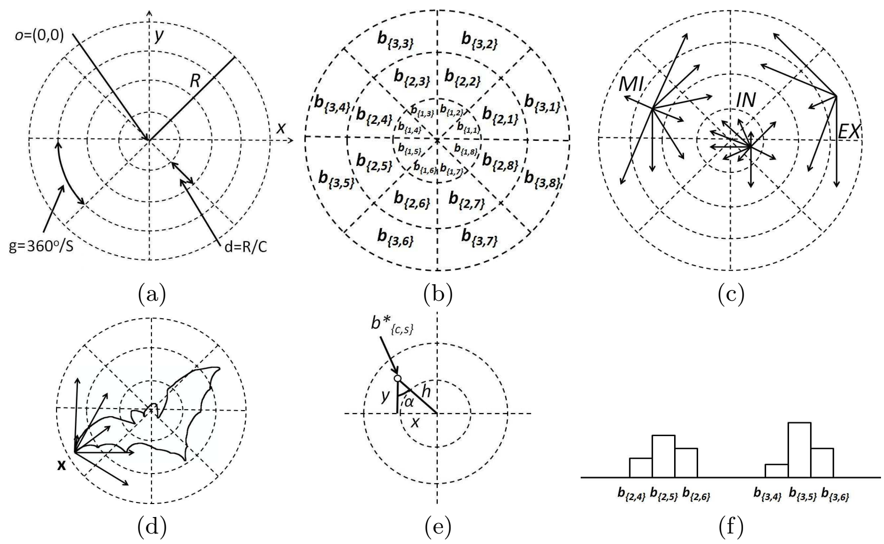


**Fig. 1.** (a) CBSM correlogram parameters, (b) regions distribution, (c) region neighbors, (d) object point analysis, (e) region centroid definition, and (f) descriptor vector update after point analysis.


**Fig. 2.** Examples of image descriptions at different sizes for two object instances.

conditions must be fulfilled: the bias induced by the zero symbol should be zero and the dynamic range of the decoding strategy must be constant for all the codewords. The complete decoding strategy weights the contribution of the decoding at each position of the codeword by the elements of $W$ that ensures that both conditions are fulfilled. As such, the final decoding strategy is defined as $d(y, T(i,\cdot)) = \sum_{j=1}^{M} W(i,j) \cdot \mathcal{L}(T(i,j) \cdot h_j(x))$, where,

$$w(i,j) = \begin{cases} r_i(S, T(\cdot, j), T(i,j)) & T(i,j) \neq 0 \\ 0 & otherwise \end{cases} \tag{1}$$

and $\sum_{j=1}^{M} W(i,j) = 1, \forall i \in \{1 \ldots K\}$. We define the meta-class relative accuracy ($r$-value) of class $k$ on the set $S$ given the following definition,

$$r_k(S, \rho, i) = \frac{\#\text{elements of class } k \text{ classified as meta-class } i \text{ in the set } S}{\#\text{elements belonging to class } k \text{ in the set } S} \tag{2}$$

where $\rho$ defines which classes belong to which meta-class.

The second part of the weighting decoding lies in a base decoding strategy. In this article, we chose to use Linear Loss-based decoding as base strategy decoding. Linear Loss-based decoding was introduced by Allwein et al. [16] and is defined in the following way: given the input sample $\mathbf{x}$ and the binary code $y$ result of applying all the dichotomizers $(h_1, h_2, \ldots, h_M)$ to the input test sample, the decoding value is defined as follows,

$$d(y, T(i, \cdot)) = \sum_{j=1}^{M} \mathcal{L}(T(i, j) \cdot h_j(x))$$

where $T(i, \cdot)$ denotes the codeword for class $i$, $h_j(x)$ is the prediction value for dichotomizer $j$, and $\mathcal{L}$ is a loss function that represents the penalty due to the miss-classification (we use $\mathcal{L}(\rho) = -\rho$).

## 4 Experimental evaluation

In order to present the results, first, we discuss the data, methods, and validation of the experiments:

• *Data*: To test the multi-class symbol recognition system, we used two multi-class data sets: the public 70-class MPEG7 repository data set [1], which contains a high number of classes with different appearance of symbols from a same class, including rotation. And secondly, a 17-class data set of grey-level symbols, which contains the common distortions from real-environments, such as illumination changes, partial occlusions, or changes in the point of view.

• *Methods*: The methods used in the comparative are: SIFT [18], Zoning, Zernique, and CSS curvature descriptors from the standard MPEG [3] [19] [20]. The details of the descriptors used for the comparatives are the followings: the optimum grid size of the CBSM descriptors is estimated applying cross-validation over the training set using a 10% of the samples to validate the different sizes of $S = \{8, 12, 16, 20, 24, 28, 32\}$ and $C\{8, 12, 16, 20, 24, 28, 32\}$. For a fair comparison among descriptors, the Zoning and BSM descriptors are set to the same number of regions than the CBSM descriptor. Concerning the Zernique technique, 7 moments are used. The length of the curve for the CSS descriptor is normalized to 200, where the $\sigma$ parameter takes an initial value of 1 and increases by 1 unit at each step. The descriptors are trained using 50 runs of Gentle Adaboost with decision stumps [9], and the one-versus-one ECOC design [16] with the Loss-Weighted decoding [17]. In order to show the benefits of the ECOC design, we also compare with a 3-Nearest Neighbor classifier.

• *Validation*: The classification score is computed by a stratified ten-fold cross-validation, testing for the 95% of the confidence interval with a two-tailed t-test.

### 4.1 MPEG7 Classification

In this experiment, we used the 70 object categories from the public MPEG7 binary object data set [1] to compare the descriptors in a multi-class categorization problem. Some examples of this data set are shown in Figure 3(a).

The classification results and confidence interval after testing using a stratified ten-fold cross-validation with a 3-NN and the ECOC configuration are shown in Table 1. Note that the best performance is obtained by our CBSM descriptor with the one-versus-one ECOC design with Loss-Weighted decoding and with 3-NN, followed by the original BSM. Moreover, the ECOC configurations always obtain higher performance than classifying with a nearest neighbor classifier.

| Descriptor | $3NN$ | ECOC Adaboost |
|---|---|---|
| CBSM | **71.84(6.73)** | **80.36(7.01)** |
| BSM | 65.79(8.03) | 77.93(7.25) |
| Zernique | 43.64(7.66) | 51.29(5.48) |
| Zoning | 58.64(10.97) | 65.50(6.64) |
| CSS | 37.01(10.76) | 44.54(7.11) |
| SIFT | 29.14(5.68) | 32.57(4.04) |

**Table 1.** Classification accuracy and confidence interval on the 70 MPEG7 symbol categories for the different descriptors using 3-Nearest Neighbor and the one-versus-one ECOC scheme with Gentle Adaboost as the base classifier.

### 4.2 Grey-scale symbol Classification

The second data set is composed by grey-level samples from 17 different classes, with a total of 550 samples acquired with a digital camera from real environments. The samples are taken so that there are high affine transformations, partial occlusions, background influence, and high illumination changes. Some examples of the 17 classes are shown in Fig. 3(b). The SIFT descriptor is a widely-used strategy for this type of images, obtaining very good results [18]. Hence, we compare the CBSM and SIFT descriptors in this experiment.

The performances and confidence intervals obtained in this experiment from a ten-fold cross-validation using the CBSM and SIFT descriptors in a one-versus-one ECOC scheme with Gentle Adaboost as the base classifier and Loss-Weighted decoding are shown in table 2. One can see that the result obtained by the CBSM descriptor adapted to grey-scale symbols significantly outperforms the result obtained by the SIFT descriptor. This difference is produced in this data set because of the high changes in the point of view of the symbols and the background influence, which significantly change the SIFT orientations.

## 5 Conclusion

In this paper, we presented the Circular Blurred Shape Model descriptor. The new descriptor is suitable to describe and recognize symbols that can suffer from

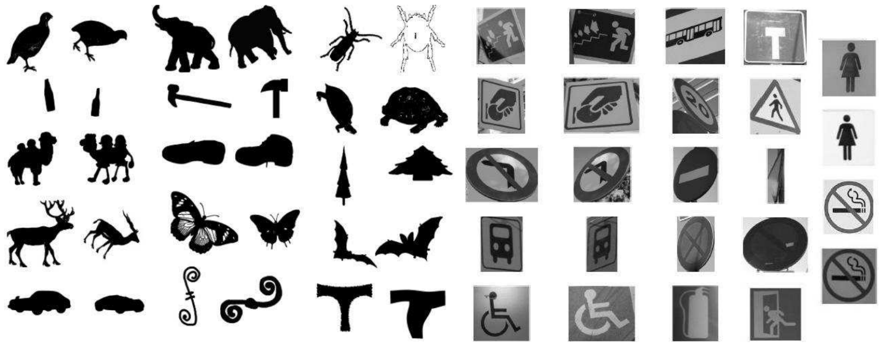

(a) (b)

**Fig. 3.** (a) MPEG samples, and (b) Grey-scale symbol data set samples.

| CBSM | SIFT |
|---|---|
| **77.82(6.45)** | 62.12(9.08) |

**Table 2.** Performance and confidence interval of the CBSM and SIFT descriptors on the grey-scale symbols data set using a one-versus-one Adaboost ECOC scheme.

several distortions, such as occlusions, rigid or elastic deformations, gaps or noise. The descriptor encodes the spatial arrangement of symbol characteristics using a correlogram structure. A prior blurring degree defines the level of degradation allowed to the symbol. Moreover, the descriptor correlogram is rotated guided by the major density so that it becomes rotationally invariant. The new symbol descriptions are learnt using Adaboost binary classifiers, and embedded in an Error-Correcting Output Codes framework to deal with multi-class categorization problems. The results over different multi-class categorization problems and comparing with the state-of-the-art descriptors show higher performance of the present methodology when classifying high number of symbol classes that suffer from irregular deformations.

## Acknowledgements

This work has been supported in part by projects TIN2006-15308-C02, TIN2006-15694-C02-02, FIS PI061290, and CONSOLIDER-INGENIO CSD 2007-00018.

## References

1. MPEG7 Repository Database, http://www.cis.temple.edu/latecki/research.html"
2. D. Zhang and G Lu, "Review of shape representation and description techniques", Pattern Recognition, vol. 37, issue 1, pp. 1-19, 2004.
3. A. Khotanzad and YH Hong, "Invariant image recognition by Zernike moments", PAMI, vol. 12, issue 5, pp. 489-497, 1990.

4. BS Manjunath, P. Salembier, and T. Sikora, "Introduction to MPEG-7: Multimedia Content Description Interface", Wiley, 2002.
5. F. Mokhtarian and A.K. Mackworth, "Scale-Based Description and Recognition of Planar Curves and Two-Dimensional Shapes", PAMI, vol. 8, n 1, pp. 34-43, 1986.
6. S. Belongie, J. Malik, and J. Puzicha, "Shape Matching and Object Recognition Using Shape Contexts", PAMI, pp. 509-522, 2002.
7. H. Bunke, "Attributed programmed graph grammars and their application to schematic diagram interpretation", PAMI, vol. 4, issue 6, pp. 574-582, 1982.
8. J. Lladós, E. Martí, and J. Villanueva, "Symbol Rec. by Error-Tolerant Subgraph Matching between Adjacency Graphs", PAMI, vol. 23(10), pp. 1137-1143, 2001.
9. J. Friedman, T. Hastie, and R. Tibshirani, "Additive logistic regression: a statistical view of boosting", Annals of Statistics, vol. 28, issue 2, pp. 337-374, 2000.
10. TG Dietterich and G. Bakiri, "Solving Multiclass Learning Problems via Error-Correcting Output Codes", JAIR, vol. 2, pp. 263-286, 1995.
11. A. Fornes, S. Escalera, J. LLados, G. Sanchez, P. Radeva, and O. Pujol, "Handwritten Symbol Recognition by a Boosted Blurred Shape Model with Error Correction", IBPRIA, vol. 4477, pp.13-21, 2007.
12. T. Dietterich and E. Kong, "Error-correcting output codes corrects bias and variance", S. Prieditis and S. Russell, ICML, pp. 313-321, 1995.
13. T. Dietterich and G. Bakiri, "Solving multiclass learning problems via error-correcting output codes", JAIR, vol. 2, pp. 263-286, 1995.
14. O. Pujol, P. Radeva, and J. Vitrià, "DECOC: A heuristic method for application dependent design of ECOC", PAMI, vol. 28, pp. 1001-1007, 2006.
15. S. Escalera, D. M. J. Tax, O. Pujol, P. Radeva, and R. P. W. Duin, "Subclass Problem-Dependent Design for Error-Correcting Output Codes", PAMI, vol. 30, issue 6, pp. 1041-1054, 2008.
16. E. Allwein, R. Schapire, and Y. Singer, "Reducing multiclass to binary: A unifying approach for margin classifiers", JMLR, vol. 1, pp. 113-141, 2002.
17. S. Escalera, O. Pujol, and P. Radeva, "On the Decoding Process in Ternary Error-Correcting Output Codes", PAMI, 2009.
18. D. Lowe, "Distinctive Image Features from Scale-Invariant Keypoints", JCV, vol. 60, issue 2, pp. 91-110, 2004.
19. W.Y.Kim and Y.S.Kim, "A new region-based shape descriptor", Hanyang University and Konan Technology, 1999.
20. Standard MPEG ISO/IEC 15938-5:2003(E)